Microscopic modeling of phonon dynamics and charge response in metallic $BaBiO_3$

Claus Falter,* Thomas Bauer, and Thomas Trautmann
Institut für Festkörpertheorie, Westfälische Wilhelms-Universität, Wilhelm-Klemm-Str. 10, 48149 Münster, Germany
(Received 9 August 2006; published 8 January 2007)

We use our recently proposed microscopic modeling in the framework of linear response theory to investigate the complete phonon dispersion, the phonon density of states, certain phonon-induced electronic charge distributions, and charge fluctuations (CF's) for anomalous soft modes of metallic $BaBiO_3$ in its simple cubic phase where superconductivity with T_c up to 32 K appears. The theoretical approach already has been applied successfully to the cuprate high-temperature superconductors, simple ionic crystals (NaCl, MgO), and perovskite oxides ($SrTiO_3$, $BaTiO_3$). It is well suited for materials with a strong component of ionic binding and especially for "ionic" metals. In particular, the giant phonon anomalies related to the breathing vibration of the oxygen as found experimentally in superconducting doped $Ba_{0.6}K_{0.4}BiO_3$, resembling those observed in the high-T_c cuprates, are investigated. The origin of these anomalies is explored and attributed to a strong nonlocal coupling of the displaced oxygen ions to CF's of ionic type, essentially of the Bi 6*s* and Bi 6*p* orbital. This points to the importance of both of these states at the Fermi energy. Starting from an *ab initio* rigid ion model we calculate the effect on the lattice dynamics and charge response of the most important electronic polarization processes in the material, i.e., CF's and dipole fluctuations. Taking into account these electronic degrees of freedom in linear response theory, we obtain a good agreement with the measured phonon dispersion and in particular with the strong phonon anomalies.

DOI: 10.1103/PhysRevB.75.014508 PACS number(s): 63.20.Dj, 74.70.−b, 74.25.Kc, 63.20.Kr

I. INTRODUCTION

Potassium doped $Ba_{1-x}K_xBiO_3$ with a transition temperature T_c up to 32 K for $x \approx 0.4$ has been intensively studied with no final resolution of its high-temperature superconductivity. Different from the cuprate high-temperature superconductors (HTSC's), its bonding is three dimensional and no antiferromagnetic ordering exists for the insulating parent compound indicating that there are no strong electronic correlations near $x=0$. Common to both materials, however, is the strong component of ionic binding favoring long-ranged Coulomb interactions and a related strong nonlocal electron-phonon coupling in terms of localized charge fluctuations (CF's) of the ionic orbitals. This type of coupling has been shown in the cuprate-HTSC's to lead to the generic phonon anomalies of the high-frequency oxygen bond-stretching modes (OBSM).[1–5] Recently, giant phonon anomalies for similar OBSM (oxygen breathing modes) also have been found by inelastic neutron scattering measurements in superconducting $Ba_{0.6}K_{0.4}BiO_3$.[7–9] Thus, while spin degrees of freedom seem to play no decisive role for superconductivity in Ba-Bi-O the effects of nonlocal coupling of lattice and charge degrees of freedom in terms of ionic CF's are still present, likewise as in the cuprate HTSC's, and provide a coupling channel for pairing in a phonon-mediated mechanism.

$Ba_{1-x}K_xBiO_3$ has a complex structural phase diagram.[10] For the insulating composition $0 \leqslant x < 0.12$ the structure is monoclinic and may be derived from the cubic perovskite structure by simultaneous octahedral tilting (*t*) and symmetric oxygen breathing-mode (*b*) distortions (frozen-in OBSM instability at the *R* point of the cubic phase). For $0.12 < x < 0.37$ the structure is still insulating but orthorhombic with a *t*, but no *b*, distortion and for the superconducting, metallic composition $(0.37 < x < 0.53)$ the structure is simple cubic, i.e., no *t* and *b* distortion.

It is widely believed that the insulating phases are generated by charge density instabilities associated with breathing and tilting distortions but it has proven difficult to establish this by first principles calculations. Recent investigations[11] indicate, in contrast to earlier results,[12] that the local-density approximation (LDA) seriously underestimates the breathing distortions and yields a metallic ground state with no sign of a charge-density-wave instability.

Moreover, first principles linear response calculations of the phonon dispersion of cubic Ba-Bi-O (Ref. 11) overestimate the high-frequency branches by about 20% in comparison with the experiments. In particular, the most strongly renormalized anomalous OBSM, O_B^R, at the *R* point, which according to the experiments[9] is found at about 10.5 THz has a frequency of 15.7 THz in the calculations presented in Ref. 11. For the modes with lower frequencies there is a better agreement of the order of 10%. Thus linear response calculations based on LDA-like electronic band structures, using a virtual-crystal approximation seem to underestimate the kinetic part of the charge response, i.e., the electronic polarizability matrix. In order to investigate this point, we study different cases for the polarizability matrix $\Pi_{\kappa\kappa'}(\mathbf{q})$ in our microscopic model approach to extract the most important electronic degrees of freedom for the charge response. The indices κ, κ' denote the orbital degrees of freedom in an elementary cell of the crystal.

Empirical shell model calculations[7–9] incorporating metallic screening by the Lindhard function are also unable to reproduce the downward dispersion and softening of the phonon anomalies; instead an upward dispersion is calculated. Finally, calculations in Ref. 13 based on a tight-binding representation of the electronic contribution to the dynamical matrix[14] and an empirical contribution for the short-ranged force constants fitted to the experimental frequencies lead to a remarkable softening for several modes

especially around the M and the R point with strongest softening for the (1, 1, 0) direction, in disagreement with the experiments where only the OBSM of breathing type are strongly renormalized and the largest softening is along the (1, 1, 1) direction.

In the present work, we calculate within our microscopic modeling of the electronic charge response in linear response theory the complete phonon dispersion, the phonon density of states, the phonon-induced electronic charge redistribution, and the CF's for the OBSM, O_B^X, O_B^M, O_B^R, of simple cubic Ba-Bi-O. In the past, this theoretical approach, which is well suited for systems with a strong component of ionic binding, has been applied successfully to the cuprate-HTSC's,[1–6] i.e., "ionic" metals in which the band crossing the Fermi level has admixture of both anion and cation orbitals, simple ionic crystals,[15] and the perovskite oxides ($SrTiO_3$, $BaTiO_3$).[16]

From a general point of view our treatment of the electronic density response and lattice dynamics in terms of dipole fluctuations (DF's) and CF's can be considered as a microscopic (semi *ab initio*) implementation of the phenomenological dipole-shell model or the charge-fluctuation models, respectively. For a general formulation of phenomenological models for lattice dynamics that use localized electronic variables as adiabatic degrees of freedom, see, for example, Ref. 17. This formulation covers shell models, bond-charge models, and charge-fluctuation models. While in such an approach the coupling coefficients are treated simply as empirical fitting parameters the essential point in our scheme is that all the couplings are microscopically well defined and can be calculated.

The ionic nature of Ba-Bi-O is described by an *ab initio* rigid ion model (RIM) leading to a local rigid charge response and electron-phonon interaction (EPI), respectively. The missing nonlocal, nonrigid part of the electronic density response and EPI is expressed by microscopically well defined CF's and DF's on the outer shells of the ions. Starting from the RIM as a reference system the effect of the nonrigid electronic polarization effects in terms of CF's and DF's on the phonon dispersion and, particularly, the anomalies is calculated and compared with the experiment.

The article is organized as follows. In Sec. II we outline the theory and modeling to provide a better reading of the article. Section III presents our calculated results of the phonon dispersion and gives a detailed discussion of the effects of screening by DF's and CF's on the phonon anomalies by comparing the corresponding results with those as obtained from the RIM as a reference system. Moreover, phonon density of states, the charge redistribution, and the CF's for the OBSM of breathing type are presented. Finally, Sec. IV contains a summary and discussion.

II. SKETCH OF THE THEORY AND MODELING

In the following, a survey of the theory and modeling is presented. A more detailed description can be found in Ref. 1 and in particular in Ref. 15 where the calculation of the microscopic coupling parameters is given. The local, rigid part of the electronic charge response and the EPI is approximated by an *ab initio* RIM taking into account ion-softening in terms of (static) effective ionic charges and scaling of the short-ranged part of certain pair potentials between the ions to simulate covalence effects in the model. This is done in such a way that the energy-minimized structure is as close as possible to the experimental one.[18] Structure optimization and energy minimization is very important for a reliable calculation of the phonon dynamics through the dynamical matrix.

The RIM with the corrections just mentioned serves as an unbiased reference system for the investigation of the effect of the nonrigid electronic polarization processes on the phonon dynamics. The latter are modeled in the form of electronic CF's on the outer shells of the ions. Especially in the metallic state the CF's dominate the nonlocal contribution of the charge response and the EPI. In addition DF's are admitted in our approach.[5,15] Thus the basic variable of our model is the ionic density which is given in the perturbed state by

$$\rho_\alpha(\mathbf{r}, Q_\lambda, \mathbf{p}_\alpha) = \rho_\alpha^0(r) + \sum_\lambda Q_\lambda \rho_\lambda^{\mathrm{CF}}(r) + \mathbf{p}_\alpha \cdot \hat{\mathbf{r}} \rho_\alpha^D(r). \quad (1)$$

ρ_α^0 is the density of the unperturbed ion, as used in the RIM, localized at the sublattice α of the crystal and moving rigidly under displacement. The Q_λ and $\rho_\lambda^{\mathrm{CF}}$ describe the amplitude and the form factors of the CF's and the last term in Eq. (1) represents the dipolar deformation of an ion α with amplitude (dipole moment) $\mathbf{p}_\alpha$ and a radial density distribution ρ_α^D. $\hat{\mathbf{r}}$ denotes the unit vector in the direction of $\mathbf{r}$. The $\rho_\lambda^{\mathrm{CF}}$ are approximated by a spherical average of the orbital densities of the ionic shells calculated in LDA taking self-interaction effects (SIC) into account. The dipole density ρ_α^D is obtained from a modified Sternheimer method in the framework of LDA-SIC.[15] All SIC calculations are performed for the average spherical shell in the orbital-averaged form according to Ref. 19. For the correlation part of the energy per electron, ϵ, the parametrization given in Ref. 19 has been used.

The total energy of the crystal is obtained by assuming that the density can be approximated by a superposition of overlapping densities ρ_α. The ρ_α^0 in Eq. (1) are also calculated within LDA-SIC taking environment effects, via a Watson-sphere potential, and the static effective charges of the ions into account. The Watson-sphere method is only used for the oxygen ions and the depth of the Watson-sphere potential is set as the Madelung potential at the corresponding site. Finally, applying the pair-potential approximation we get the total energy

$$E(R, \zeta) = \sum_{\mathbf{a},\alpha} E_\alpha^{\mathbf{a}}(\zeta) + \frac{1}{2} \sum_{(\mathbf{a},\alpha)\neq(\mathbf{b},\beta)} \Phi_{\alpha\beta}(\mathbf{R}_\beta^{\mathbf{b}} - \mathbf{R}_\alpha^{\mathbf{a}}, \zeta). \quad (2)$$

The energy E depends on both the configuration of the ions $\{R\}$ and the electronic (charge) degrees of freedom (EDF) $\{\zeta\}$ of the charge density, i.e., $\{Q_\lambda\}$ and $\{\mathbf{p}_\alpha\}$ in Eq. (1). $E_\alpha^{\mathbf{a}}$ are the energies of the single ions. $\mathbf{a}$, $\mathbf{b}$ denote the elementary cells and α, β the corresponding sublattices. The second term in Eq. (2) is the interaction energy of the system expressed in terms of anisotropic pair interactions $\Phi_{\alpha\beta}$. Both $E_\alpha^{\mathbf{a}}$ and $\Phi_{\alpha\beta}$ in general depend upon ζ via ρ_α in Eq. (1).

The pair potentials in Eq. (2) can be separated into long-ranged Coulomb contributions and short-ranged terms as follows:

$$\Phi_{\alpha\beta}(\mathbf{R},\zeta) = \frac{\mathcal{Z}_\alpha \mathcal{Z}_\beta}{R} - (\mathcal{Z}_\alpha \mathbf{p}_\beta + \mathcal{Z}_\beta \mathbf{p}_\alpha)\frac{\mathbf{R}}{R^3} + \frac{\mathbf{p}_\alpha \cdot \mathbf{p}_\beta}{R^3} - 3\frac{(\mathbf{p}_\alpha \cdot \mathbf{R})(\mathbf{R} \cdot \mathbf{p}_\beta)}{R^5} + \tilde{\Phi}_{\alpha\beta}(\mathbf{R},\zeta), \tag{3}$$

$$\tilde{\Phi}_{\alpha\beta}(\mathbf{R},\zeta) = K_\alpha U_\beta(\mathbf{R},\zeta) + K_\beta U_\alpha(\mathbf{R},\zeta) + W_{\alpha\beta}(\mathbf{R},\zeta) + G_{\alpha\beta}(\mathbf{R},\zeta). \tag{4}$$

The first term in Eq. (3) describes the long-ranged ion-ion, the second the dipole-ion, and the third and fourth term the dipole-dipole interaction. $\mathcal{Z}_\alpha$ and $\mathcal{Z}_\beta$ are the variable charges of the ions in case CF's are excited. The latter reduce to the ionic charges for rigid ions. K_α and K_β are the charges of the ion cores. $\tilde{\Phi}_{\alpha\beta}$ represents the short-ranged interactions. These can be expressed by the following integrals:

$$U_\alpha(\mathbf{R},\zeta) = -\int d^3r \rho_\alpha(\mathbf{r},\zeta)\left(\frac{1}{|\mathbf{r}-\mathbf{R}|} - \frac{1}{R} - \frac{\mathbf{r}\cdot\mathbf{R}}{R^3}\right), \tag{5}$$

$$W_{\alpha\beta}(\mathbf{R},\zeta) = \int d^3r \int d^3r' \left[\rho_\alpha(\mathbf{r},\zeta)\rho_\beta(\mathbf{r}',\zeta)\left(\frac{1}{|\mathbf{r}-\mathbf{r}'-\mathbf{R}|} - \frac{1}{R} - \frac{(\mathbf{r}+\mathbf{r}')\cdot\mathbf{R}}{R^3}\right)\right], \tag{6}$$

$$G_{\alpha\beta}(\mathbf{R},\zeta) = \int d^3r[\rho_{\alpha\beta}(\mathbf{r},\zeta)\epsilon(\rho_{\alpha\beta}(\mathbf{r},\zeta)) - \rho_\alpha(\mathbf{r},\zeta)\epsilon(\rho_\alpha(\mathbf{r},\zeta)) - \rho_\beta(\mathbf{r}-\mathbf{R},\zeta)\epsilon(\rho_\beta(\mathbf{r}-\mathbf{R},\zeta))], \tag{7}$$

with

$$\rho_{\alpha\beta}(\mathbf{r},\zeta) = \rho_\alpha(\mathbf{r},\zeta) + \rho_\beta(\mathbf{r}-\mathbf{R},\zeta). \tag{8}$$

$K_\alpha U_\beta(\mathbf{R},\zeta)$ yields the short-ranged contribution of the interaction between the core α and the density ρ_β according to Eq. (1). $W_{\alpha\beta}(\mathbf{R},\zeta)$ represents the short-ranged Coulomb contribution of the interaction of the density ρ_α with the density ρ_β and $G_{\alpha\beta}(\mathbf{R},\zeta)$ is the sum of the kinetic one-particle and exchange-correlation contribution of the interaction between the two ions.[15] The short-ranged part of the potentials and the various coupling coefficients are calculated numerically for a set of distances R between the ions. The results so obtained are then described by an analytical function of the form

$$f(R) = \pm\exp\left(\alpha + \beta R + \frac{\gamma}{R}\right). \tag{9}$$

α, β, and γ in Eq. (9) are fit parameters.

From the adiabatic condition

$$\frac{\partial E(R,\zeta)}{\partial \zeta} = 0 \tag{10}$$

an expression for the atomic force constants and accordingly the dynamical matrix in harmonic approximation consistent with linear response theory can be derived:

$$t_{ij}^{\alpha\beta}(\mathbf{q}) = [t_{ij}^{\alpha\beta}(\mathbf{q})]_{\mathrm{RIM}} - \frac{1}{\sqrt{M_\alpha M_\beta}}\sum_{\kappa,\kappa'}[B_i^{\kappa\alpha}(\mathbf{q})]^*[C^{-1}(\mathbf{q})]_{\kappa\kappa'}B_j^{\kappa'\beta}(\mathbf{q}). \tag{11}$$

The first term on the right-hand side denotes the contribution from the RIM. M_α, M_β are the masses of the ions and $\mathbf{q}$ is a wave vector from the first Brillouin zone. The quantities $\mathbf{B}(\mathbf{q})$ and $C(\mathbf{q})$ in Eq. (11) represent the Fourier transforms of the electronic coupling coefficients as calculated from the energy in Eq. (2), and the pair potentials in Eqs. (3)–(8), respectively:

$$\mathbf{B}_{\kappa\beta}^{\mathbf{ab}} = \frac{\partial^2 E(R,\zeta)}{\partial\zeta_\kappa^{\mathbf{a}}\partial R_\beta^{\mathbf{b}}}, \tag{12}$$

$$C_{\kappa\kappa'}^{\mathbf{ab}} = \frac{\partial^2 E(R,\zeta)}{\partial\zeta_\kappa^{\mathbf{a}}\partial\zeta_{\kappa'}^{\mathbf{b}}}. \tag{13}$$

κ denotes the EDF (CF and DF in the present model) in an elementary cell. The $\mathbf{B}$ coefficients describe the coupling between the EDF and the displaced ions (bare electron-phonon coupling), and the coefficients C determine the interaction between the EDF. The phonon frequencies, $\omega_\sigma(\mathbf{q})$, and the corresponding eigenvectors, $\mathbf{e}^\alpha(\mathbf{q}\sigma)$, of the modes $(\mathbf{q}\sigma)$ are obtained from the secular equation for the dynamical matrix in Eq. (11), i.e.,

$$\sum_{\beta,j} t_{ij}^{\alpha\beta}(\mathbf{q})e_j^\beta(\mathbf{q}) = \omega^2(\mathbf{q})e_i^\alpha(\mathbf{q}). \tag{14}$$

The lengthy details of the calculation of $\mathbf{B}$ and C cannot be reviewed in this paper. They are given in Ref. 15. In this context we remark that the coupling matrix $C_{\kappa\kappa'}(\mathbf{q})$ of the EDF-EDF interaction, whose inverse appears in Eq. (11) for the dynamical matrix, can be written in matrix notation as

$$C = \Pi^{-1} + \tilde{V}. \tag{15}$$

Π^{-1} contains the kinetic single particle contribution to the interaction C and $\tilde{V}$, the Hartree and exchange-correlation contribution. C^{-1} is needed for the dynamical matrix and the EPI is closely related to the (linear) density response function (matrix) and to the inverse dielectric function (matrix) ε^{-1}, respectively. Comparing with calculations of the phonon dispersion and the EPI using the linear response method in the form of density functional perturbation theory within local density approximation (LDA), these calculations correspond to calculating Π and $\tilde{V}$ in DFT-LDA. On the other hand, in our microscopic modeling DFT-LDA-SIC calculations are performed for the various densities in Eq. (1) in order to obtain the coupling coefficients $\mathbf{B}$ and $\tilde{V}$. SIC as a correction for a single particle term is important for contracting in particular localized orbitals. Written in matrix notation we get for the density response matrix the relation

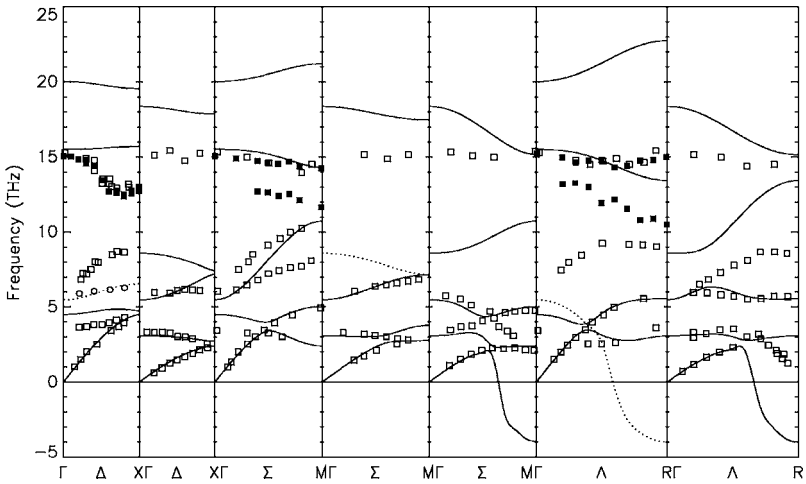

FIG. 1. Calculated phonon dispersion of Ba-Bi-O in the cubic perovskite structure in the main symmetry directions $\Delta \sim (0,0,1)$, $\Sigma \sim (1,1,0)$, and $\Lambda \sim (1,1,1)$ for the ionic reference model with covalent corrections (RIM, model 1). The open symbols represent the experimental results for cubic $Ba_{0.6}K_{0.4}BiO_3$ (Ref. 7). The full squares are experimental results of the same material (Ref. 9). The arrangement of the panels from left to right according to different irreducible representations is as follows: $|\Delta_1(—),\Delta_2(\cdots)|\Delta_3(—)|\Sigma_1(—)|\Sigma_2(—),\Sigma_3(\cdots)||\Sigma_4(—)|\Lambda_1(—),\ \Lambda_2(\cdots)|\Lambda_3(—)|$. The measured anomalous soft oxygen-breathing vibrations at the X, M, and R point show the following frequencies: $O_B^X \approx 12.8$ THz, $O_B^M \approx 11.8$ THz, and $O_B^R \approx 10.5$ THz, respectively. Imaginary frequencies of unstable modes are represented as negative numbers.

$$C^{-1} = \Pi(1 + \tilde{V}\Pi)^{-1} \equiv \Pi\varepsilon^{-1}, \quad \varepsilon = 1 + \tilde{V}\Pi. \tag{16}$$

The CF-CF submatrix of the matrix Π can, for example, be approximated from a tight-binding approximation of a single particle electronic band structure. In this case the electronic polarizability Π reads

$$\Pi_{\kappa\kappa'}(\mathbf{q},\omega=0) = -\frac{2}{N}\sum_{n,n',\mathbf{k}} \frac{f_{n'}(\mathbf{k}+\mathbf{q}) - f_n(\mathbf{k})}{E_{n'}(\mathbf{k}+\mathbf{q}) - E_n(\mathbf{k})} \times [C^*_{\kappa n}(\mathbf{k}) C_{\kappa n'}(\mathbf{k}+\mathbf{q})] \times [C^*_{\kappa' n}(\mathbf{k}) C_{\kappa' n'}(\mathbf{k}+\mathbf{q})]^*. \tag{17}$$

f, E, and C in Eq. (17) are the occupation numbers, the single-particle energies, and the expansion coefficients of the Bloch functions in terms of tight-binding functions.

As a measure of the strength of the EPI the self-consistent change of an EDF on an ion, induced by a phonon mode $(\mathbf{q},\sigma)$, can be derived in the form

$$\delta\zeta^{\mathbf{a}}_\kappa(\mathbf{q}\sigma) = \left[-\sum_\alpha \mathbf{X}^{\kappa\alpha}(\mathbf{q})\mathbf{u}_\alpha(\mathbf{q}\sigma)\right] e^{i\mathbf{q}\mathbf{R}^{\mathbf{a}}_\kappa} \equiv \delta\zeta_\kappa(\mathbf{q}\sigma) e^{i\mathbf{q}\mathbf{R}^{\mathbf{a}}}, \tag{18}$$

with the displacement of the ions

$$\mathbf{u}^{\mathbf{a}}_\alpha(\mathbf{q}\sigma) = \left(\frac{\hbar}{2M_\alpha\omega_\sigma(\mathbf{q})}\right)^{1/2} \mathbf{e}^\alpha(\mathbf{q}\sigma) e^{i\mathbf{q}\mathbf{R}^{\mathbf{a}}} \equiv \mathbf{u}_\alpha(\mathbf{q}\sigma) e^{i\mathbf{q}\mathbf{R}^{\mathbf{a}}}. \tag{19}$$

The quantity $\mathbf{X}$ in Eq. (18), i.e., the self-consistent response per unit displacement of the EDF, is calculated in linear response theory as

$$\mathbf{X}(\mathbf{q}) = \Pi(\mathbf{q})\varepsilon^{-1}(\mathbf{q})\mathbf{B}(\mathbf{q}) = C^{-1}(\mathbf{q})\mathbf{B}(\mathbf{q}). \tag{20}$$

Another measure of the EPI for a certain phonon mode $(\mathbf{q}\sigma)$ is provided by the change of the self-consistent potential in the crystal felt by an electron at a space point $\mathbf{r}$, i.e., $\delta V_{\text{eff}}(\mathbf{r},\mathbf{q}\sigma)$. Averaging this quantity with the corresponding density form factor $\rho_\kappa(\mathbf{r}-\mathbf{R}^{\mathbf{a}}_\kappa)$ of the EDF located at $\mathbf{R}^{\mathbf{a}}_\kappa$, we obtain

$$\delta V^{\mathbf{a}}_\kappa(\mathbf{q}\sigma) = \int dV \rho_\kappa(\mathbf{r}-\mathbf{R}^{\mathbf{a}}_\kappa)\delta V_{\text{eff}}(\mathbf{r},\mathbf{q}\sigma). \tag{21}$$

This gives an orbital resolved measure for the strength of the EPI in the mode $(\mathbf{q}\sigma)$ mediated by the EDF considered. For an expression of $\delta V^{\mathbf{a}}_\kappa(\mathbf{q}\sigma)$ in terms of coupling coefficients in Eqs. (12) and (13), see Ref. 20.

III. RESULTS AND DISCUSSION

A. Results within the reference system (RIM)

The rigid, local contribution of the electronic charge response and EPI is approximated by an *ab initio* RIM with corrections for covalence effects in terms of effective ionic charges (ion softening) and scaling of the short-ranged pair potential between the Bi and oxygen ion. In this way, we obtain a suitable reference system; see Fig. 1 for the calculated dispersion, which subsequently allows for the investigation of the characteristic nonrigid screening effects in terms of CF's and DF's on the phonon dispersion and charge response.

The covalent corrections are important because a calculation of the phonon dispersion of cubic Ba-Bi-O with nominal charges leads to a significant overestimation of the width of the phonon spectrum. Moreover, various unstable modes down to −12 THz emerge if imaginary frequencies of un-

stable modes are represented as negative numbers. The mode with the highest frequency (≈35 THz) in such a model is the oxygen-breathing mode, O_B^R, at the R point which, on the other hand, according to recent experiments[9] is anomalously soft (≈10.5 THz); see Fig. 1. Similar results are found in calculations of the phonon dispersion of cuprate high-temperature superconductors when nominal ionic changes are used.[1,21] In our calculation we find a set of effective (static) ionic charges (Ba 1.5+, Bi 2.7+, O 1.4−) and a covalent scaling of the Bi-O pair potential which leads to an energy minimized structure in full agreement with the experimental one for cubic Ba-Bi-O (a=4.2742 Å).[10] As a general rule, partial covalence reduces the amplitude of the static ionic charges in mixed ionic-covalent compounds like Ba-Bi-O, because the charge transfer from the cations to the anions is not complete as in the entirely ionic case.

The phonon dispersion based on this set of reduced ionic charges is displayed in Fig. 1 (model 1). Potassium doping is taken into account using a virtual-mass approximation and implicitly via the reduced static charges. The phonon dispersion calculated with such a reference model means a large improvement compared to the model with nominal charges (not shown). In particular, the width of the spectrum is considerably reduced and compares well with the experiments if the missing renormalization related to the nonrigid charge response (CF's and DF's) is taken into account; see Sec. III B. Moreover, unstable modes only appear at the R and M point. The mode at R is triply degenerate and represents rotations around any cubic axis. The rotation is opposite in neighboring elementary cells in all cubic directions. The other unstable mode at M is similar to the most unstable R point mode, with the exception that the rotation of the octahedra is in the same sense in adjacent cells along the z axis. Note in this context that, as mentioned in the Introduction, the structural phase transitions in K-doped Ba-Bi-O are characterized by rotations (tilts) of the BiO_6 octahedra around several distinct axes[10] and in cubic $Ba_{0.6}K_{0.4}BiO_3$ the frequency of the rotational R point mode is extremely low (Fig. 1), consistent with the tendency of soft rotational modes at R in harmonic theory. Thus our results within the harmonic approximation highlight the importance of the ionic forces for the tilt instabilities and indicate that anharmonic contributions should stabilize these modes. Frozen-phonon calculations support this argument because they predict highly anharmonic potential behavior for the tilting of the BiO_6 octahedra corresponding to the R point.[11,22]

In $SrTiO_3$ the rotational modes at R also are found most unstable in our calculations[16] corresponding to an antiferrodistortive transition in agreement with the experiment while our calculation for $BaTiO_3$ finds the ferroelectric mode at Γ as the most unstable one again in accordance with the experimental situation. Interestingly, we also obtain, in the case of the HTSC La_2CuO_4,[18,20] one partially unstable branch with the tilt mode at the X point. Freezing in of this distortion points correctly to the experimentally observed structural phase transition from the high-temperature tetragonal to the low-temperature orthorhombic structure. Again this rotational instability is already present in the RIM and thus also driven by the long-ranged ionic interactions likewise as in Ba-Bi-O and Sr-Ti-O. In contrast to the situation in Ba-Ti-O

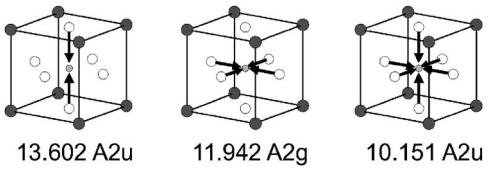

FIG. 2. Displacement patterns of the anomalous oxygen-breathing modes O_B^X, O_B^M, and O_B^R from left to right for model 3. Frequencies are given in units of THz.

the strongly polar ferroelectric TO mode at Γ, where the oxygen anions vibrate coherently in the opposite direction to the Bi ion, is stable in Ba-Bi-O. We get 8.6 THz in the RIM with effective ionic charges and 9.7 THz in the RIM with nominal ones. Not only is the frequency of the ferroelectric mode significantly reduced when passing from the model with nominal ionic charges to the model with effective charges but the LO-TO mode splittings are also. On inspection of Fig. 1 with respect to the oxygen-breathing modes, displayed in Fig. 2, we find that instead of being soft as in the experiment the latter have the highest frequency at the $X(O_B^X)$, $M(O_B^M)$, and $R(O_B^R)$ point, respectively. Consequently, the characteristic downward dispersion of the anomalous phonon branches cannot be described at all within the RIM, i.e., by a rigid, local charge response. In the following, we will show that the anomalous dispersion and phonon softening characteristic for cubic, metallic Ba-Bi-O is essentially related to strong nonlocal, nonrigid EPI effects mediated by CF's of the Bi 6s and Bi 6p orbitals, pointing to a substantial character also of Bi 6p electrons in the electronic state near the Fermi energy.

B. The effects of a nonrigid, nonlocal charge response via CFs and DFs

Starting from the reference systems (RIM) of the last subsection DF's and CF's as nonrigid electronic degrees of freedom are additionally allowed for the modeling. This means that on each ion the electrons can redistribute under atomic displacements in such a way that dipole and charge fluctuations are induced on that ion in order to minimize the energy.

In Fig. 3 we display our calculated results of the phonon dispersion taking additional DF's into account (model 2). In this calculation the *ab initio* values of the dipole polarizability α as calculated from the Sternheimer method in the framework of DFT-LDA-SIC (Ref. 15) for the corresponding single ions are reduced by 50% which leads to a better agreement of the phonon dispersion with the experiment. Taking the *ab initio* values for α as calculated for the single ions with the Sternheimer method overestimates the dipole polarization in the crystalline environment and leads to TO frequencies being low as compared to the experiment. These findings also hold true for our calculations of dipole screening in the cuprate based HTSC's,[5,23] where in addition the dipole polarizability is found to be very anisotropic dominating along the (ionic) c direction.

Comparing Fig. 3 with Fig. 1 we find that the width of the spectrum improves considerably and no additional unstable branches emerge. Moreover, the LO-TO splittings are further

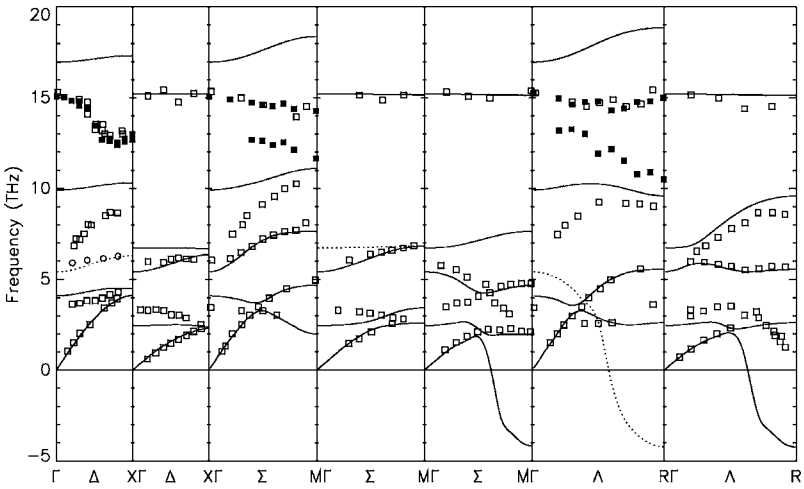

FIG. 3. Same as in Fig. 1 with the calculated results from the model described in the text where in addition to the RIM (model 1) dipole fluctuations are taken into account (model 2).

reduced and the TO modes are well described. In particular, the ferroelectronic TO mode at Γ is reduced from 8.6 to 6.7 THz and is now in quite good agreement with experiment.[7,8] However, the anomalous branches with the oxygen-breathing modes at *X*, *M*, and *R* have an increasing dispersion when propagating from the Γ point towards the zone boundary and show no sign of softening. Likewise as in the RIM, these modes have the highest frequencies in the spectrum.

Next, we discuss the influence of the ionic CF's on the phonon dispersion. The results of a calculation where, in addition to DF's (model 2), CF's are included are shown in Fig. 4 (model 3). Comparing the calculated results with the experiments a good agreement is now achieved. This is particularly true for the phonon anomalies which cannot be described well by other approaches up to now as stated in the Introduction. First principle calculations[11] within DFT-LDA for Ba-Bi-O taking K doping into account by a virtual-crystal and virtual-mass approximation report that the breathing distortions are seriously underestimated in the LDA. These calculations yield for the O_B^R mode a frequency of 15.7 THz compared to 10.5 THz in the experiment.[9] We argue in the following that a reason for the high frequency in this calculation is the electronic polarizability $\Pi_{\kappa\kappa'}(\mathbf{q})$ from Eq. (17), i.e., the kinetic single particle part of the charge response, which seems underestimated in LDA-type calculations as in Ref. 11 or Ref. 24, respectively.

In order to investigate this question in our approach, $\Pi_{\kappa\kappa'}(\mathbf{q})$ is modeled in an appropriate way to find out which electronic degrees of freedom are most important for the phonon anomalies in Ba-Bi-O. So, we express $\Pi_{\kappa\kappa'}(\mathbf{q})$ in Fourier-transformed (parametrized) form

$$\Pi_{\kappa\kappa'}(\mathbf{q}) = \sum_{\mathbf{a}} \Pi_{\kappa\kappa'}^{\mathbf{0a}} e^{i\mathbf{q}(\mathbf{R}_{\kappa'}^{\mathbf{a}} - \mathbf{R}_{\kappa})}. \tag{22}$$

In the metallic phase the electronic partial density of states (PDOS) at the Fermi level $Z_\kappa(\varepsilon_F)$ is related to the polarizability matrix in the long wavelength limit[1,3] according to

$$\sum_{\kappa'} \Pi_{\kappa\kappa'}(\mathbf{q} \to \mathbf{0}) = Z_\kappa(\varepsilon_F), \tag{23}$$

and the total density of states at energy ε is given by

$$Z(\varepsilon) = \sum_{\kappa} Z_\kappa(\varepsilon). \tag{24}$$

In our calculations for the metallic phase of the cuprate HTSC's we have found[3,5,6] that neglecting the $\mathbf{q}$ dependence in the polarizability and taking into account the diagonal on-site parameters $\Pi_{\kappa\kappa}^{\mathbf{00}}$ alone already provides a good approximation for the calculation of the phonon dispersion, in particular for the anomalous generic OBSM in these materials. This means that the parameters $\Pi_{\kappa\kappa}^{\mathbf{00}}$ are approximated by

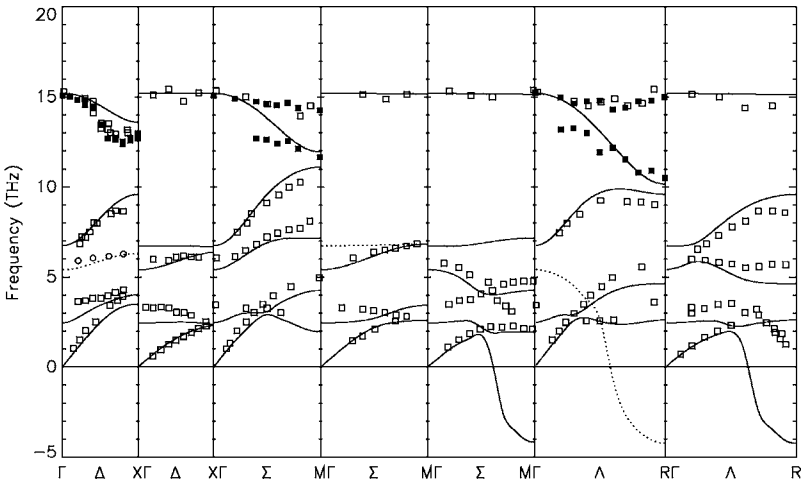

FIG. 4. Same as in Fig. 1 with the calculated results from the model described in the text where in addition to the RIM dipole and charge fluctuations are included (model 3).

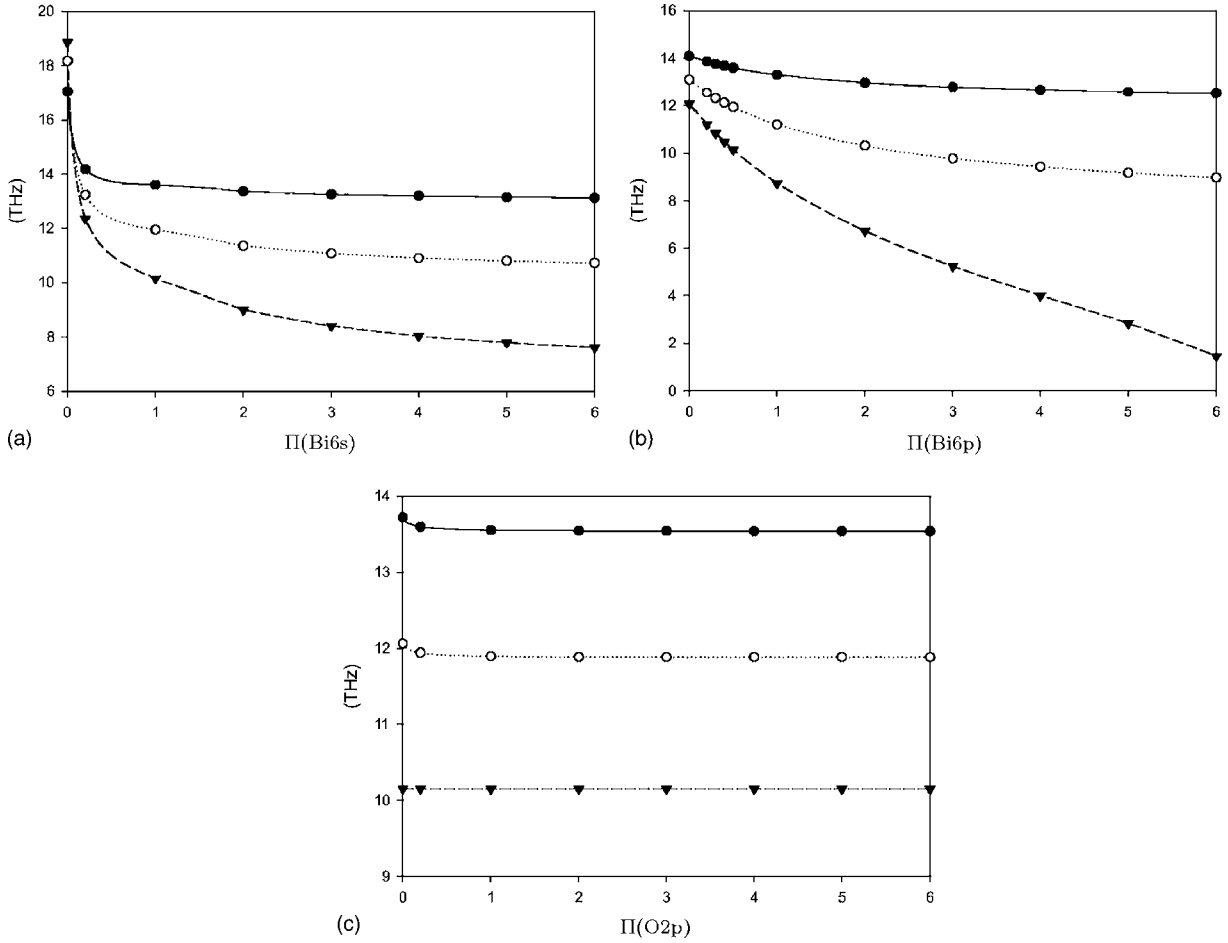

FIG. 5. Calculated effect of the Bi 6s, Bi 6p, and O 2p charge fluctuations on the softening of the frequency of the anomalous oxygen bond-stretching (breathing) modes O_B^X, O_B^M, and O_B^R, respectively, for varying polarizabilities Π(Bi 6s), Π(Bi 6p), and Π(O 2p). Π is given in eV^{-1}. X point (full line), M point (dotted line), and R point (broken line).

the corresponding PDOS. However, such a diagonal approximation does not hold for the insulating state of a material. Due to the charge gap in the spectrum off-site elements $\Pi^{0a}_{\kappa\kappa'}$ necessarily must occur and interfere in such a way that the following compressibility sum rules for the kinetic single particle part of the charge response are satisfied:[1,3,6]

$$\sum_{\kappa'} \Pi_{\kappa\kappa'}(\mathbf{q} \to \mathbf{0}) = O(q), \tag{25}$$

$$\sum_{\kappa\kappa'} \Pi_{\kappa\kappa'}(\mathbf{q} \to \mathbf{0}) = O(q^2). \tag{26}$$

In Fig. 5 we display the calculated effect of the Bi 6s, Bi 6p, and O 2p charge fluctuations for the softening of the frequency of the anomalous OBSM O_B^X, O_B^M, and O_B^R, respectively, by varying the diagonal on-site parameters Π(Bi 6s) $=Z_{\text{Bi }6s}(\varepsilon_F)$, Π(Bi 6p)$=Z_{\text{Bi }6p}(\varepsilon_F)$, and Π(O 2p)$=Z_{\text{O }2p}(\varepsilon_F)$. We find that the CF's in the Bi 6s and Bi 6p orbitals both are important for the phonon softening, while the dependence on the O 2p CF's is very weak. The values actually chosen for the calculation of the phonon dispersion in model 3 are Π(Bi 6s)$=1.00$ eV^{-1}, Π(Bi 6p)$=0.5$ eV^{-1}, and Π(O 2p) $=0.2$ eV^{-1}. The latter value, to a large extent irrelevant for the softening, was taken to optimize the phonon frequencies for modes where exclusively O 2p CF's are excited. The remarkable softening with increasing $Z_{\text{Bi }6p}(\varepsilon_F)$ indicates that the band crossing the Fermi energy consists not only of the Bi 6s and O 2p electrons but also has a substantial admixture of Bi 6p electrons. This is also concluded from electronic band structure calculations, see Ref. 11 and references therein, and is consistent with the static effective charge for Bi in our model pointing out a partial occupation of the Bi 6p orbital. The latter is the most delocalized one of the orbitals used in our calculation (see Fig. 6) and consequently very effective for screening and softening of the oxygen bond-stretching vibrations.

Such an enhancement of softening, related to the delocalized components of the electronic state at the Fermi energy, also has been obtained in our calculations of the generic anomalous OBSM in the cuprate HTSC's. In this case we have shown that with increased hole doping the inclusion of the delocalized Cu 4s state into the orbital basis is an important factor for the strength of the anomalies in the optimally and overdoped state.[2,6,20] Thus doping (similar like pressure) causes a progressive modification of the orbital character of the electronic state in the cuprate-HTSC's. Quite generally,

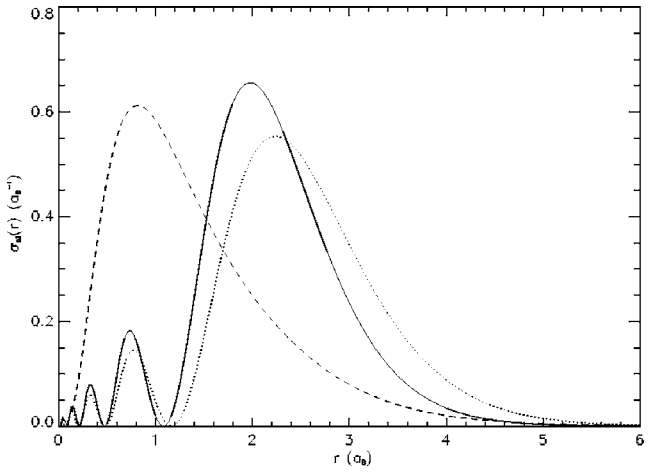

FIG. 6. Charge density form factors (times $4\pi r^2$) for the $Bi^{2.7+}$ and $O^{1.4-}$ ion. r radial distance in units of a_B. Bi $6s$ (full curve); Bi $6p$ (dotted curve); O $2p$ (broken curve).

our investigations in the cuprates point to an interrelation between electronic structure changes at ε_F, selective phonon softening via strong nonlocal EPI of CF type, and, finally, to the appearance of phonon-mediated superconductivity in an "ionic" metal. A corresponding connection seems also to hold in doped Ba-Bi-O.

A change of the electronic state in Ba-Bi-O, i.e., a partial shift of the spectral weight from Bi $6s$ to Bi $6p$, as suggested from our calculations of the OBSM, obviously occurs parallel with K doping because the OBSM anomalies are not present in the weakly doped material.[8] It has been argued in Ref. 25 that K doping creates localized holes on the O $2p$ orbitals, rather than on Bi atoms. One might speculate that an increased population of the Bi $6p$ states as the most delocalized ones lowers the energy by an enhanced hybridization with the O $2p$ hole states making the latter itinerant at a certain doping level in the metallic state.

An increasing Bi $6p$ character of the electronic state at ε_F also should lead from a more rounded Fermi surface to a more distorted anisotropic shape. Such a change of the geometry of the Fermi surface would of course be mapped to the "phase space factor" (nesting function) and also to the matrix elements of the electron-phonon spectral function $\alpha^2F(\omega)$ and, finally, to the superconducting T_c in a phonon-mediated mechanism.

Altogether from our results a multiorbital model involving CF's, DF's, and the corresponding interactions $\tilde{V}$ in the charge response, Eqs. (15) and (16), between Bi $6s$, Bi $6p$, and O $2p$ states is needed to obtain a reliable description of the phonon dispersion in an "ionic" metal like Ba-Bi-O, as shown in Fig. 4.

Comparing the results of the dispersion in Figs. 3 and 4 we recognize that the LO-TO splittings at Γ are closed by the metallic screening due to the CF's. Such a screening of the long wavelength polar modes does not imply charge localization on a microscopic scale and can also be achieved in a homogeneous electron gas model. However, localization of charge on a microscopic scale is necessary for the screening of the zone-boundary modes like O_B^X, O_B^M, and O_B^R. In this case, nonlocally induced ionic Bi $6s$ and Bi $6p$ CF's lead to the strong softening. Compare with Fig. 7, where the nonlocal part of the phonon-induced charge density redistribution is shown for O_B^X, O_B^M, and O_B^R. The related strong softening of the modes by the nonlocally excited nonrigid charge response via CF's and DF's as compared to the RIM can be extracted from Fig. 8.

In context with the vanishing of the LO-TO splitting characteristic phonon branches along Δ, Σ, and Λ with the (stable) ferroelectric TO mode at Γ (6.744 THz) appear in the phonon dispersion which are well described in our model. Even details, like the steep slopes near Γ, resulting from the depression of the LO frequency by metallic screening, and the flattening out of the branch in Λ direction, is obtained in our calculation.

In order to investigate the question of how the phonon dispersion looks, if we use an electronic density of states at ε_F for Ba-Bi-O which is typical for a LDA-like calculation[24] in our model for the polarizability, we have performed the

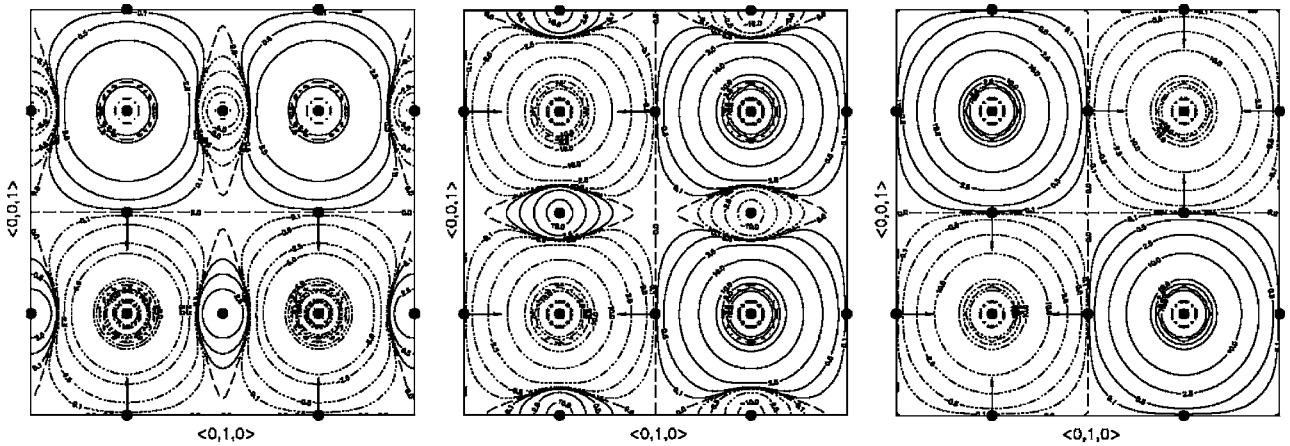

FIG. 7. Contour plot of the nonlocal part of the phonon-induced charge density redistribution from Eq. (27) for (a) the O_B^X mode, (b) the O_B^M mode, and (c) the O_B^R mode in model 3. The units are $10^{-4}/a_B^3$. Full lines (—) describe regions of space where electrons are attracted and the lines (—···) represent regions where electrons are pushed away.

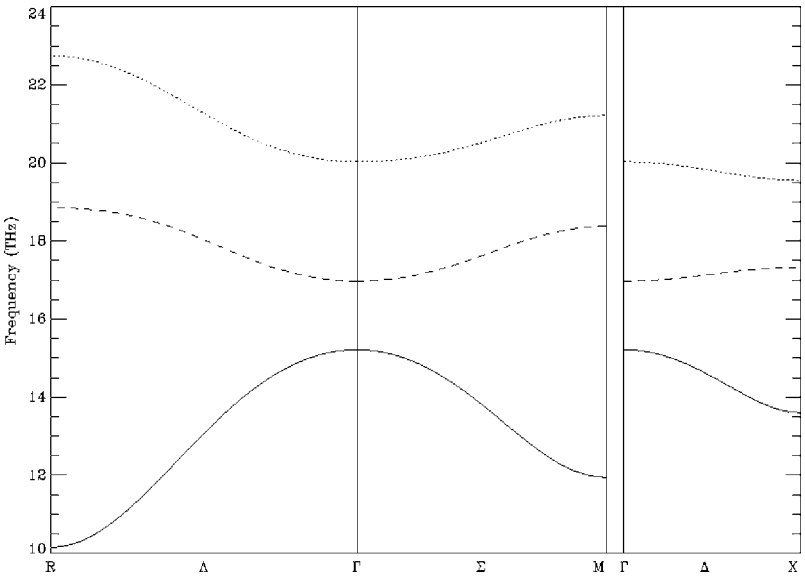

FIG. 8. Calculated anomalous branches with the oxygen-breathing modes O_B^X, O_B^M, and O_B^R as end points of the $\Delta\sim(0,0,1)$, $\Sigma\sim(1,1,0)$, and $\Lambda\sim(1,1,1)$ direction, respectively. The line type $(\cdots)$ denotes the result for the RIM (model 1), (---) additionally includes DF's (model 2), and the full lines represent the final calculation including DF's and CF's (model 3).

calculations shown in Fig. 9. The total density of states from Ref. 24 is 0.8 eV^{-1}. Taking for $\Pi(O\,2p)$ the same value as in model 3 and using the same ratio for $\Pi(Bi\,6s)$ and $\Pi(Bi\,6p)$ we obtain $\Pi(Bi\,6s)=0.4\ eV^{-1}$, $\Pi(Bi\,6p)=0.2\ eV^{-1}$, and $\Pi(O\,2p)=0.2\ eV^{-1}$ (model 4). Comparing the results for model 4 in Fig. 9 with those in Fig. 4 we find that the softening of the oxygen-breathing mode anomalies is only poorly developed, consistent with the *ab initio* calculations based on DFT-LDA in Ref. 11. This indicates that the *ab initio* LDA calculations underestimate the EPI for the OBSM.

The underestimation of the EPI in the breathing modes can also be deduced from Table I in terms of the CF's. Here the CF's according to Eq. (18) of the Bi $6s$, Bi $6p$, and O $2p$ orbitals generated by O_B^X, O_B^M, and O_B^R are listed. We recognize that in our modeling of the electronic state with enhanced PDOS for Bi $6s$ and Bi $6p$ at ε_F as compared to the LDA-based result the CF's are significantly larger leading to the correct description of the anomalies in the phonon dispersion.

The strong nonlocal EPI of ionic CF type in the oxygen-breathing modes is also illustrated in the contour plots of the nonlocal part of the phonon-induced charge density redistribution $\delta\rho(\mathbf{r},\mathbf{q}\sigma)$ for the OBSM in Fig. 7, i.e.,

$$\delta\rho(\mathbf{r},\mathbf{q}\sigma)=\sum_{\mathbf{a},\kappa}\delta\zeta_\kappa^{\mathbf{a}}(\mathbf{q}\sigma)\rho_\kappa(\mathbf{r}-\mathbf{R}_\kappa^{\mathbf{a}}),\tag{27}$$

with the CF's $\delta\zeta_\kappa^{\mathbf{a}}$ according to Eq. (18) and the form factors ρ_κ for the CF's as in Eq. (1). The total phonon-induced charge redistribution can be obtained by adding the rigid displacement of the unperturbed densities, i.e.,

$$\delta\rho_r(\mathbf{r},\mathbf{q}\sigma)=\sum_{\mathbf{a},\alpha}\{\rho_\alpha^0(\mathbf{r}-[\mathbf{R}_\alpha^{\mathbf{a}}+\mathbf{u}_\alpha^{\mathbf{a}}(\mathbf{q}\sigma)])-\rho_\alpha^0(\mathbf{r}-\mathbf{R}_\alpha^{\mathbf{a}})\}.\tag{28}$$

ρ_α^0 is the density of the unperturbed ion from Eq. (1) and $\mathbf{u}_\alpha^{\mathbf{a}}$ the displacement of an ion in Eq. (19).

The results shown in Fig. 7 demonstrate that the nonlocal EPI leads to attractive (—) and repulsive (— ··) regions for electrons mainly at the Bi ions. For symmetry reasons some charge is also transferred to the silent oxygens in the O_B^X and O_B^M mode; see Figs. 7(a) and 7(b) and Table I. This, however, is not possible in O_B^R because all the oxygen ions are vibrating symmetrically toward or away from Bi. Electrons, i.e., negative charge, are flowing to the expanded octahedra from

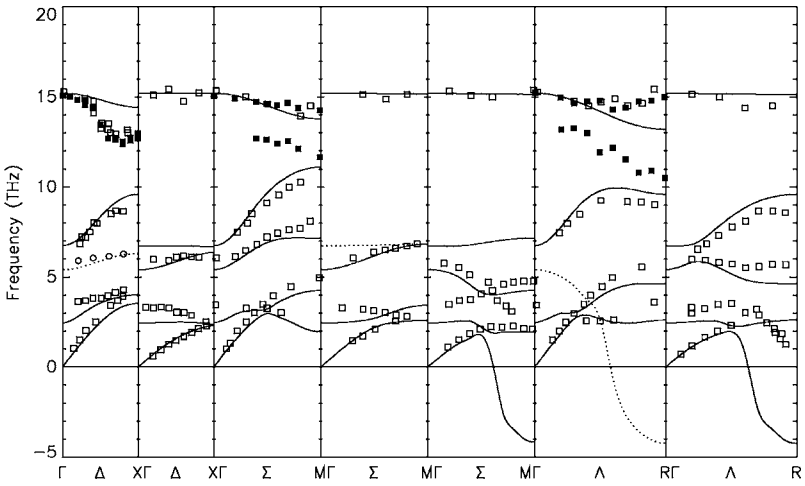

FIG. 9. Same as in Fig. 1 with the calculated results from the model described in the text where in addition to the RIM dipole fluctuations and charge fluctuations are included. The latter are based on a model where an electronic density of states at ε_F typical for LDA calculations of Ba-Bi-O (Ref. 24) is used (model 4).

TABLE I. Calculated phonon-induced charge fluctuation $\delta\zeta_\kappa(\mathbf{q}\sigma)$ for model 3 (first row) and model 4 (second row) for O_B^X, O_B^M, and O_B^R according to Eq. (18). Units are in 10^{-3} electrons. $\delta\zeta_\kappa(\mathbf{q}\sigma)>0$ means that electrons are pushed away. The symbol "/" means that no CF's are excited.

	$\delta\zeta_{\text{Bi }6s}$	$\delta\zeta_{\text{Bi }6p}$	$\delta\zeta_{\text{O }2p}$
O_B^X	39.369	27.534	−4.169
	32.333	18.285	−1.764
O_B^M	61.329	42.740	−5.791
	46.309	26.227	−2.092
O_B^R	83.657	57.859	/
	56.807	32.220	/

the compressed ones. Thus negative charge is always accumulated in the larger octahedra and so a (dynamical) charge disproportionation of the Bi ions is generated. The corresponding CF's of the Bi 6*s*, Bi 6*p*, and O 2*p* orbitals $\delta\zeta_\kappa(\mathbf{q}\sigma)$ for O_B^X, O_B^M, and O_B^R are collected in Table I. Significantly larger values are found for model 3 compared with the LDA-based model 4. For example, in the O_B^R mode 0.142 electrons are exchanged between the vibrating octahedra in model 3 and only 0.089 electrons in model 4. For lightly K-doped insulating Ba-Bi-O besides the tilt distortion related to the rotational modes there is also a breathing distortion (frozen-in breathing mode) of the octahedra. On the other hand, our calculations in model 3 for the metallic phase show that strong nonlocal EPI of CF type lead to a large softening but a still stable O_B^R breathing mode in very good agreement with experiment. However, the result indicates that this type of nonlocal EPI also should play a role for the actual breathing distortion in the insulating part of the phase diagram. One can interpret the $\delta\rho$ patterns in Fig. 7 and the CF's in Table I as an expression of a precursor effect for polaron formation. Actually, polarons are not expected to form at a high enough doping level, because, as mentioned before, the system can gain sufficient energy by delocalization via the hybridization of the Bi 6*s* and in particular the Bi 6*p* states with the O 2*p* hole states created by doping. However, such a channel for a lowering of the energy by delocalization might not be favorable in the insulating, lightly doped material due to the small number of holes and the tilted structure where the O 2*p* to Bi 6*p* hopping is decreased due to misalignment of the orbitals and hence the energy gain by delocalization. In this case (polaronic) charge localization by the strong nonlocal EPI of CF type might be energetically more favorable and responsible for the metal-insulator transition. A tendency to polaron formation is also very likely in the undoped and weakly doped cuprate-HTSC's, where our modeling of the charge response has shown that the delocalized component of the electronic state, i.e., in this case Cu 4*s*, is not required to describe the phonon anomalies in these "phases" of the cuprates.[2,3,6,20] Polaronic effects also occur in the small nonadiabatic region around the *c* axis of the cuprate HTSC's, where an insulatorlike charge response and phonon-plasmon mixing is found.[20,26] As a matter of fact, the electronic structure of the lightly K-doped insulating phase of Ba-Bi-O is

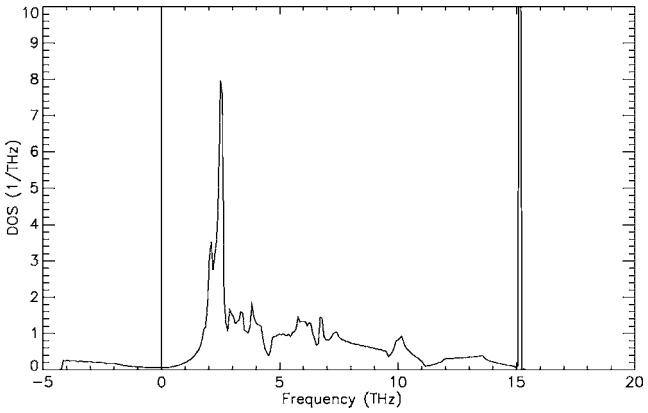

FIG. 10. Phonon density of states (DOS) for cubic Ba-Bi-O as calculated with model 3, including CF's and DF's.

not really understood. However, as discussed, e.g., in Refs. 27 and 28 and from our discussion formation of small polaron or bipolarons due to strong nonlocal EPI may be an important mechanism for insulating behavior persisting over a wide doping range.

The mode splitting experimentally found in recent experiments for the anomalous branches along Σ and Λ for metallic Ba-Bi-O (Ref. 9) (see the full symbols in the figures of the phonon dispersion) cannot be understood in calculations assuming an ideal cubic perovskite symmetry. As discussed in Ref. 9 the split dispersion suggests some charge inhomogeneity due to distortions from the cubic perovskite structure on a time scale larger than the time scale of the phonons. For example, a structural tilt distortion around the cubic (0, 0, 1) direction recently reported for superconducting Ba-Bi-O (Ref. 29) should lead to an increase of the OBSM at the *M* and *R* point because of the reduced O 2*p* to Bi 6*p* hopping due to misalignment of the orbitals and a corresponding reduction of the softening via Bi 6*p*.

Anomalous phonon softening and mode splitting of the oxygen bond-stretching phonon along (1, 0, 0), most likely due to a (dynamic) charge inhomogeneity, very recently also has been observed in La-Ba-Cu-O.[30] As discussed in Ref. 6 a charge inhomogeneity should lead locally to a variation of the strength of the nonlocal EPI of CF type and a related variation of the phonon frequency of the OBSM. How the phonon frequency is changed depends in particular on the state of the inhomogeneity which could be compressible or incompressible or a mixture of both. In a phonon-mediated pairing mechanism such a variation of the nonlocal EPI by inhomogeneity is expected to induce simultaneously a corresponding change of the pairing strength (gap value) and a variation of the frequency of the pairing related modes. Stronger renormalized modes (lower frequencies), i.e., a stronger nonlocal EPI, correlates to a larger pairing strength (higher gap value), and vice versa. Interestingly, such a correlation has been observed quite recently in scanning tunneling experiments in $Bi_2Sr_2CaCu_2O_8$.[31]

In the last topic of this paper we present calculations for the phonon density of states within model 3 including CF's and DF's; see Fig. 10. Moreover, in Fig. 11 the calculated atom-resolved phonon density of states is shown. Concern-

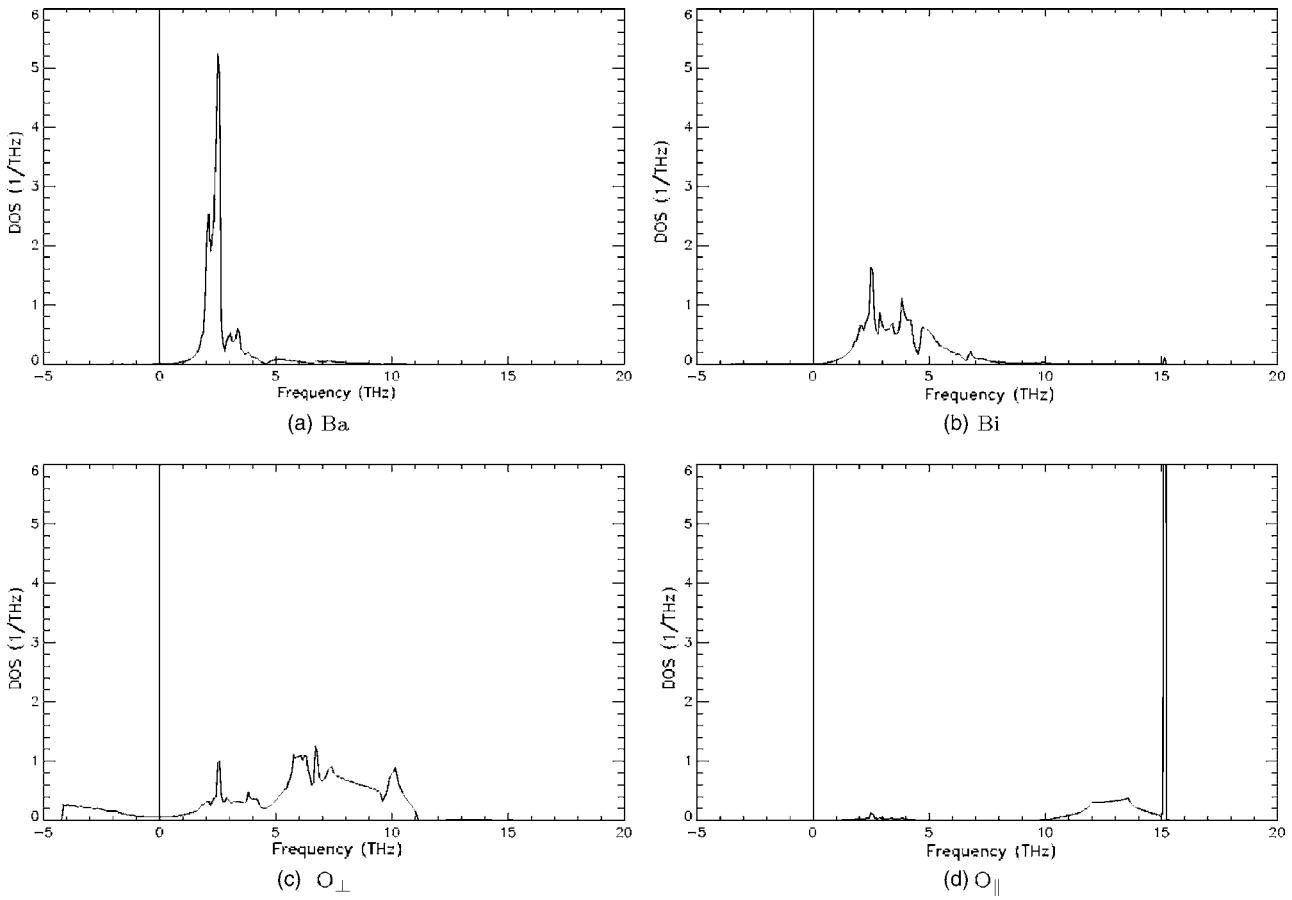

FIG. 11. Partial phonon density of states calulated with model 3. (a) Ba-DOS; (b) Bi-DOS; (c) $O_\perp$-DOS; (d) $O_\parallel$-DOS. The symbol $\parallel$ or $\perp$, respectively, means parallel or perpendicular to the Bi-O bond.

ing the oxygen ion we have further discriminated between displacements parallel ($O_\parallel$) and perpendicular ($O_\perp$) with respect to the Bi-O bond in order to demonstrate the strongly anisotropic behavior of the oxygen vibrations in Ba-Bi-O.

From the figures we see that the frequency range up to about 5 THz can be attributed to Ba and Bi vibrations with some contribution from $O_\perp$ including the unstable rotational modes. The $O_\perp$ vibrations dominate the spectral range from around 5 THz to about 11 THz. Beyond this frequency range the high-frequency part from 10–15 THz is exclusively governed by the $O_\parallel$ vibrations including the von Hove points of the OBSM: $O_B^X \approx 13.6$ THz, $O_B^M \approx 11.9$ THz, and $O_B^R \approx 10.2$ THz. The anisotropy between the $O_\parallel$ and $O_\perp$ vibrations will, for example, be reflected in the Debye-Waller factors. The latter are expected to be considerably larger perpendicular to the Bi-O bond in agreement with experiments[10] and consistent with a tendency towards a structural phase transition via rotational modes. Finally, the strong almost singular peak at about 15 THz results from the characteristic nearly dispersionless branches in Fig. 4 terminating at the Γ point in the TO mode with the highest frequency.

IV. SUMMARY AND DISCUSSION

Within our microscopic modeling of the electronic charge response in linear response theory we have studied complete phonon dispersion curves, phonon-induced charge density redistributions and charge fluctuations, generated by nonlocal EPI, and the total and atom-resolved phonon density of states in cubic metallic Ba-Bi-O. Our calculated results of the phonon dispersion curves are in good overall agreement with the experiments; in particular, the strong phonon softening of the anomalous oxygen-breathing modes is well described. This was not possible so far neither with empirical nor with *ab initio* calculations based on the LDA using a virtual crystal approximation. The latter seem to underestimate the kinetic single particle part of the density response. Increasing the electronic PDOS for the Bi 6*s* and Bi 6*p* orbitals at the Fermi level as compared with typical values obtained in LDA calculations has been shown to provide the strong softening of the OBSM. This is achieved by a characteristic type of local screening on a microscopic scale in terms of ionic CF's being quite generally at work in "ionic" metals with a significant component of ionic binding like Ba-Bi-O or the cuprate based HTSC's. More explicitly, nonlocal coupling of the displaced oxygen ions in the OBSM essentially to Bi 6*s* and Bi 6*p* CF's, which are favored by the corresponding large PDOS of these states at ε_F, are found to be responsible for the softening.

The effect of the strong nonlocal EPI is also visible from the calculation of the nonlocal part of the charge density redistribution and the CF's themselves during the oxygen vibrations in the octahedra. Accordingly, a considerable (dy-

namical) charge disproportionation has been calculated. The patterns of charge rearrangement can be looked upon as a visualization of a precursor effect for polaron formation. Small polaron and/or bipolaron formation is very likely an important mechanism for the insulating behavior in lightly K-doped Ba-Bi-O.

The strong effect for softening by including the Bi $6p$ orbitals into the electronic state at the Fermi energy points towards a change of this state with K doping. This change is accompanied by a corresponding variation of the topology of the Fermi surface and possible changes of the electron-phonon matrix elements. Both effects are important for the electron-phonon spectral function $\alpha^2F(\omega)$ and the T_c value in a phonon-mediated mechanism for superconductivity. Such a mechanism is supported by the strong nonlocal EPI effects found in our calculations. Compared with the cuprate based HTSC spin degrees of freedom seem to play no role for superconductivity in Ba-Bi-O but the strong nonlocal mode-selective coupling effects of lattice and charge degrees of freedom in terms of ionic CF's are present in both Ba-Bi-O and the cuprate HTSC's.

From our calculations of the PDOS of the phonons we extract that the oxygen vibrations and consequently also the mean square displacements are very anisotropic. There are low-frequency $O_\perp$ vibrations perpendicular to the Bi-O bond which are well separated from the high-frequency $O_\parallel$ vibrations parallel to the bond.

Quite generally, our investigations for metallic Ba-Bi-O and the cuprate-HTSC's point to an interrelation between doping induced electronic structure changes at the Fermi energy, selective phonon softening via strong nonlocal EPI of CF type, and high-temperature superconductivity in "ionic" metals.

*Email address: falter@nwz.uni-muenster.de

[1] C. Falter, M. Klenner, and W. Ludwig, Phys. Rev. B **47**, 5390 (1993).
[2] C. Falter, M. Klenner, G. A. Hoffmann, and Q. Chen, Phys. Rev. B **55**, 3308 (1997).
[3] C. Falter and G. A. Hoffmann, Phys. Rev. B **61**, 14537 (2000).
[4] C. Falter and G. A. Hoffmann, Phys. Rev. B **64**, 054516 (2001).
[5] C. Falter and F. Schnetgöke, Phys. Rev. B **65**, 054510 (2002).
[6] C. Falter, Th. Bauer, and F. Schnetgöke, Phys. Rev. B **73**, 224502 (2006).
[7] M. Braden, W. Reichardt, W. Schmidbauer, A. S. Ivanov, and A. Y. Rumiantsev, J. Supercond. **8**, 595 (1995).
[8] M. Braden, W. Reichardt, A. S. Ivanov, and A. Y. Rumiantsev, Europhys. Lett. **34**, 531 (1996).
[9] M. Braden, W. Reichardt, S. Shiryaev, and S. N. Barilo, Physica C **378-381**, 89 (2002).
[10] S. Pei, J. D. Jorgensen, B. Dabrowski, D. G. Hinks, D. R. Richards, A. W. Mitchell, J. M. Newsam, S. K. Sinha, D. Vaknin, and A. J. Jacobson, Phys. Rev. B **41**, 4126 (1990).
[11] V. Meregalli and S. Y. Savrasov, Phys. Rev. B **57**, 14453 (1998).
[12] A. I. Liechtenstein, I. I. Mazin, C. O. Rodriguez, O. Jepsen, O. K. Andersen, and M. Methfessel, Phys. Rev. B **44**, 5388 (1991).
[13] M. Shirai, N. Suzuki, and K. Motizuki, J. Phys.: Condens. Matter **2**, 3553 (1990).
[14] C. M. Varma and W. Weber, Phys. Rev. B **19**, 6142 (1979).
[15] C. Falter, M. Klenner, G. A. Hoffmann, and F. Schnetgöke, Phys. Rev. B **60**, 12051 (1999).
[16] Th. Trautmann and C. Falter, J. Phys.: Condens. Matter **16**, 5955 (2004).
[17] P. B. Allen, Phys. Rev. B **16**, 5139 (1977).
[18] C. Falter, M. Klenner, and G. A. Hoffmann, Phys. Rev. B **52**, 3702 (1995).
[19] J. P. Perdew and A. Zunger, Phys. Rev. B **23**, 5048 (1981).
[20] C. Falter, Phys. Status Solidi B **242**, 78 (2005).
[21] R. E. Cohen, W. E. Pickett, L. L. Boyer, and H. Krakauer, Phys. Rev. Lett. **60**, 817 (1988).
[22] K. Kunc and R. Zeyher, Phys. Rev. B **49**, 12216 (1994).
[23] C. Falter and F. Schnetgöke, J. Phys.: Condens. Matter **15**, 8495 (2003).
[24] L. F. Mattheiss and D. R. Hamann, Phys. Rev. Lett. **60**, 2681 (1988).
[25] S. Salem-Sugui, E. E. Alp, S. M. Mini, M. Ramanathan, J. C. Campuzano, G. Jennings, M. Faiz, S. Pei, B. Dabrowski, Y. Zheng, D. R. Richards, and D. G. Hinks, Phys. Rev. B **43**, 5511 (1991).
[26] C. Falter, G. A. Hoffmann, and F. Schnetgöke, J. Phys.: Condens. Matter **14**, 3239 (2002).
[27] I. B. Bischofs, V. N. Kostur, and P. B. Allen, Phys. Rev. B **65**, 115112 (2002).
[28] T. Nishio, J. Ahmad, and H. Uwe, Phys. Rev. Lett. **95**, 176403 (2005).
[29] M. Braden, W. Reichardt, E. Elkaim, J. P. Lauriat, S. Shiryaev, and S. N. Barilo, Phys. Rev. B **62**, 6708 (2000).
[30] D. Reznik, L. Pintschovius, M. Ito, S. Iikubo, M. Sato, H. Goka, M. Fujita, K. Yamada, G. D. Gu, and J. M. Tranquada, Nature (London) **440**, 1170 (2006).
[31] J. Lee, K. Fujita, K. McElroy, J. A. Slezak, M. Wang, Y. Aiura, H. Bando, M. Ishikado, T. Masui, J. X. Zhu, A. V. Balatsky, H. Eisaki, S. Uchida, and J. C. Davis, Nature (London) **442**, 546 (2006).